



Synthesis and solid state structure of oxacalix[4]arenes bearing four nitro groups and four *tert*-butyl groups at their extra-annular positions

Shuichiro Akagi, Yusuke Yasukawa, Kazuhiro Kobayashi, Hisatoshi Konishi*

Department of Chemistry and Biotechnology, Graduate School of Engineering, Tottori University, 4-101 Koyama-minami, Tottori, Tottori 680-8552, Japan

ARTICLE INFO

Article history:

Received 23 July 2009

Received in revised form

30 September 2009

Accepted 30 September 2009

Available online 2 October 2009

ABSTRACT

Four oxacalix[4]arene derivatives, in which 1,3-dinitrobenzene units and 1,3-di-*tert*-butylbenzene units are incorporated in alternating order, were synthesized by aromatic nucleophilic substitution. The introduction of the *tert*-butyl groups increased the stability of the macrocycles against nucleophilic C–O bond cleavage. X-ray crystal structure analyses reveal that the oxacalixarenes adopt an unsymmetrical 1,3-alternate conformation. The bulky substituents did not disturb the conjugation between the bridging oxygen atoms and the dinitrobenzene rings.

© 2009 Elsevier Ltd. All rights reserved.

1. Introduction

Oxacalixarenes are oxygen-atom-bridged metacyclophane compounds. In contrast to classical calixarenes connected by carbon atoms to bridge their aromatic rings, the incorporation of oxygen atoms within the metacyclophane framework is an interesting method of increasing structural diversity and conferring new chemical and physical properties upon this class of molecules.¹ These macrocycles are usually obtained by base-catalyzed aromatic nucleophilic substitution of activated dihalogenated aromatic or heteroaromatic compounds with dihydroxyaromatic compounds.² The rigid structure makes oxacalixarenes attractive as a building block for the construction of supramolecular architectures.³

We previously reported^{2c} that CsF-catalyzed aromatic nucleophilic substitution of 1,3-difluoro-4,6-dinitrobenzene **1** with 2-propylresorcinol **2** initially produced three cyclic products, *syn*-cyclic tetramer *syn*-**3**, *anti*-cyclic tetramer *anti*-**3**, and cyclic hexamer **4** in moderate yields (Scheme 1). After longer reaction times, however, the amount of the *anti*-**3** and **4** decreases. Finally, only *syn*-**3** was obtained in good yield. These results suggest that the *anti*-**3** and **4** are the kinetic products and that they convert to *syn*-**3** under the reaction conditions for their formation. Furthermore, the reversibility of the C–O bond formation was confirmed by reconstruction of both *anti*-**3** and **4** to *syn*-**3** in the presence of CsF.

It is noteworthy that the cyclization reaction is not suppressed by the introduction of the intra-annular substituents. This fact is postulated to be a result of the preferred conformation of the *syn*-isomers. Thus, X-ray analysis of the tetranitrooxacalix[4]arenes

bearing no substituents at the intra-annular positions indicated that in the crystal the cyclic tetramers adopt a 1,3-alternate (or a boat) conformation with the resorcinol rings oriented nearly perpendicular to the mean planes defined by the bridging oxygen atoms. These conformational features are very similar to those of the oxacalix[4]arenes bearing propyl^{2c} or methyl⁴ substituents at the intra-annular positions as schematically shown in Scheme 1. Comparison of these conformations suggests that there is no severe steric hindrance between the alkyl substituents at the intra-annular positions and the neighboring dinitrobenzene rings. Hence, the *syn*-cyclic tetramers were obtained as the thermodynamically most stable products.

In continuation of our interests in the design and synthesis of oxacalixarenes, we report here the synthesis of oxacalix[4]arene bearing bulky alkyl substituents at their extra-annular positions. The present work was conducted to test whether the preference of an oxacalix[4]arene for the cyclic tetramer formation can be modified by the presence of substituents at the 4,6-positions of the resorcinol units. Here we describe the synthesis and solid state structure of oxacalix[4]arenes **6** bearing four nitro groups and four *tert*-butyl groups at their extra-annular positions.

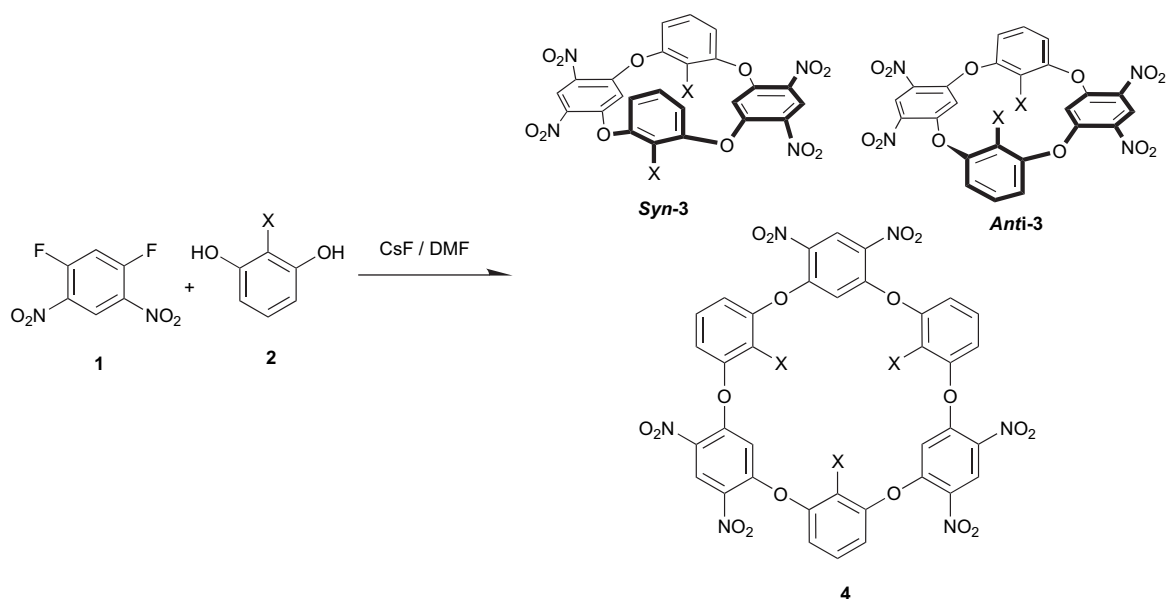
2. Result and discussion

2.1. Synthesis

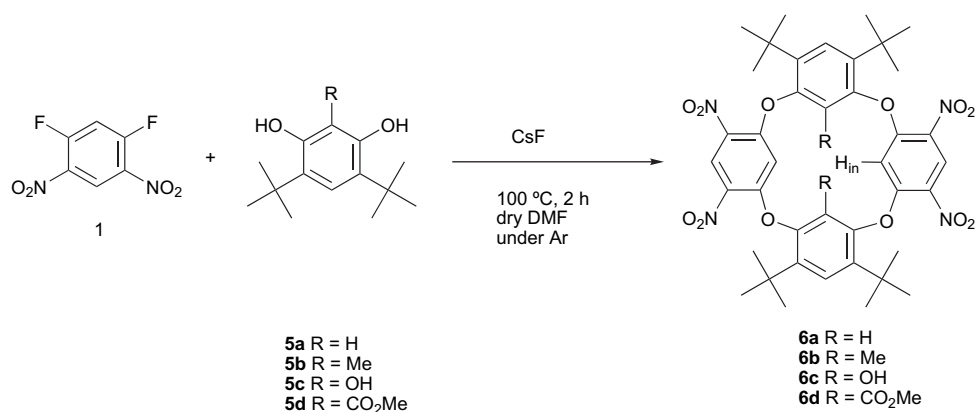
The resorcinols **5a–d** bearing two *tert*-butyl substituents at their 4,6-positions were used for construction of the oxacalix[4]arenes. The CsF-catalyzed aromatic nucleophilic substitution of 1,5-difluoro-2,4-dinitrobenzene **1** with **5a** was conducted in DMF at 100 °C for 2 h (Scheme 2). The crude product was purified by recycling preparative gel permeation chromatography (GPC) to produce the cyclic

* Corresponding author.

E-mail address: konis@chem.tottori-u.ac.jp (H. Konishi).



Scheme 1. Synthesis of oxacalix[*n*]arenes bearing substituents at their intra-annular positions by aromatic nucleophilic substitution.



Scheme 2. Synthesis of oxacalix[4]arenes **6** from 4,6-di-*tert*-butylresorcinols **5**.

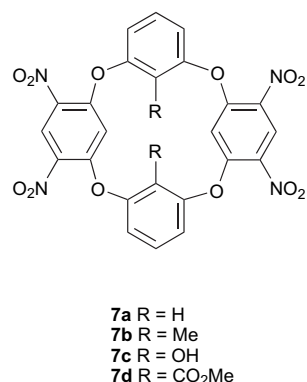
tetramer **6**. These structures were confirmed by ¹H and ¹³C NMR spectroscopies, infrared spectrometry, elemental analysis, and conclusively identified by X-ray structure determinations. Their yields and the chemical shifts of the intra-annular aromatic protons on the dinitrobenzene rings (H_{in}, see Scheme 2) are summarized in Table 1. The chemical shifts of the H_{in} protons (5.65–6.16 ppm) indicate that these protons are significantly affected by the ring current of the neighboring di-*tert*-butylbenzene rings. Thus, it can be presumed that the preferred conformations of **6** are estimated to be 1,3-alternate similar to those observed in the crystal structure (vide infra).

Table 1
The yields of oxacalix[4]arenes **6** and the chemical shifts of their H_{in} protons in CDCl₃

Compound	R	Yield (%)	H _{in} (ppm)
6a	H	74	6.16
6b	Me	70	5.73
6c	OH	27	6.00
6d	CO ₂ Me	49	5.65

Despite the presence of bulky *tert*-butyl groups at the *ortho* positions, the cyclic tetramer **6a** was synthesized by the reaction of **1** with **5a** in 74% yield. Furthermore, no evidence of the presence of oxacalix[6]arene in the reaction mixture was obtained. It appears

that the bulky groups bonded to the 4,6-positions of the resorcinol units hinder the formation of the oxacalix[6]arene. Meanwhile, it was reported^{3b} that steric hindrance may also be one of the reasons for the formation of larger macrocycles in the oxacalix[4]arene synthesis, where bulky groups were substituted at the 5-positions of the resorcinol units. The C–O bond of tetranitrooxacalix[4]arenes, for example **7** (Scheme 3), is readily cleaved by the *ipso*-attack



Scheme 3. Tetranitrooxacalix[4]arenes bearing no bulky substituents at their extra-annular positions.

Table 2

MM3⁺ calculated steric energy differences between the *syn*- and *anti*-isomer of oxacalix[4]arenes

Compound	ΔE (kJ mol ⁻¹)	Compound	ΔE (kJ mol ⁻¹)
6a	65.98	7a	9.57
6b	53.38	7b	6.43
6c	61.29	7c	15.06
6d	71.61	7d	11.99

of nucleophiles.^{3c,5} In contrast, **6a** is stable to alkaline hydrolysis by 5% KOH in THF/H₂O (9:1). We also found that the reconstruction of oxacalix[4]arene **6a** with resorcinol in the presence of CsF in DMF did not occur. These observations indicate that the C–O bond formation of **6a** is irreversible in the present study. Furthermore, it seems that the bulky *tert*-groups hinder the approach of nucleophiles and destabilize the transition state for ring cleavage.

The reaction of **1** with **5b** also produced the oxacalix[4]arene **6b** (*syn*-isomer) in good yield (70%), and the corresponding *anti*-isomer could not be obtained by GPC separation of the reaction mixture. When 2-methylresorcinol **2** (X=Me) was used as a resorcinol unit, two conformational isomers, *syn*-**3** (X=Me) and *anti*-**3** (X=Me), were obtained.⁴ Because of these isomers do not practically interconvert with each other at the reaction temperature (100 °C), it is reasonably concluded that the reaction of **1** with **5b** produced only one stereoisomer, *syn*-**6b**. The dihydroxyoxacalix[4]arene **6c** was obtained in a low yield (27%). GPC analysis of the reaction mixture indicated the formation of a large amount of a complex mixture with higher molecular weights. ¹H NMR analysis of this fraction indicated the formation of a mixture of the linear and/or branched higher oligomers. Similar results were obtained in K₂CO₃/DMSO or the Et₃N/MeCN system. This is in contrast to the facile synthesis of the dihydroxy derivative, *syn*-**3** (X=OH), which was prepared in

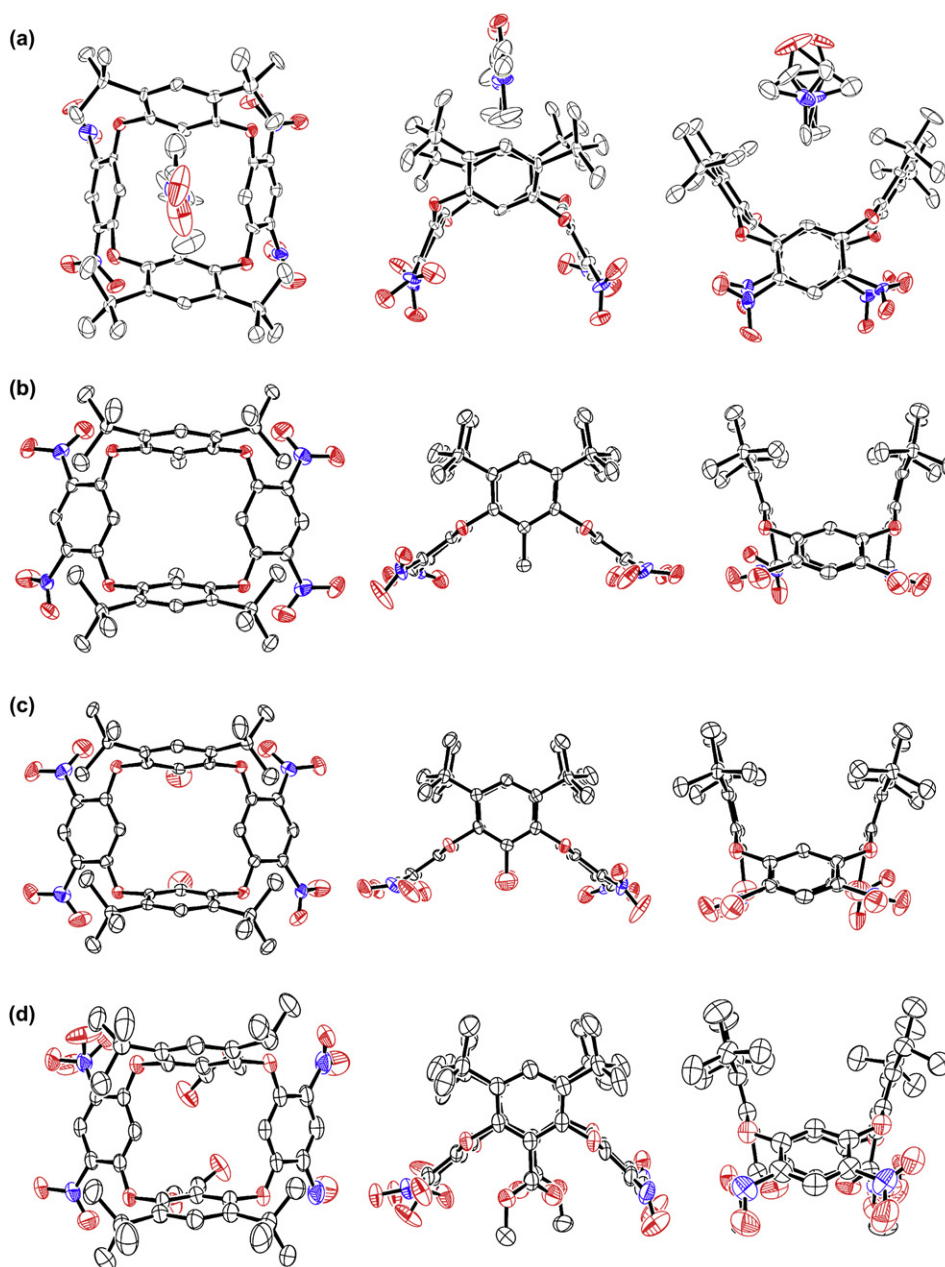


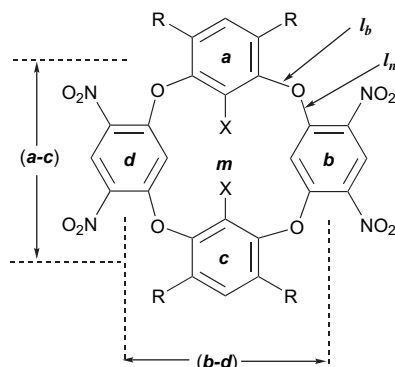
Figure 1. Molecular structures of **6a–d**, top and side views. Thermal ellipsoids are drawn 50% probability level. Atom coloring: O, red; N, blue. Hydrogen atoms are omitted for clarity. (a) **6a**, the DMF molecule is disordered with a ratio 1:1 occupancy; (b) **6b**; (c) **6c**; (d) **6d**, one nitro group is disordered in two parts, solvent molecules are omitted for clarity.

$K_2CO_3/DMSO^{3a}$ in good yield. The low yield of **6c** might be due to the adjacent *tert*-butyl groups, which reduce the regioselectivity of the hydroxyl groups at 1- and 3-positions of **5c**. The diester derivative **6d** was prepared in rather poor yield (49%). In this case, only the *syn*-isomer was also separated by GPC. The alkaline hydrolysis of the ester groups was examined. However, we have found that the ester groups are stable in 5% KOH in THF/H₂O (9:1) under reflux conditions. This low reactivity may be due to protection of the ester groups by the neighboring aromatic rings at both sides in the 1,3-alternate conformation.

To assess the stereoselectivities of the *syn*- and *anti*-isomers, molecular mechanics calculations using the MacroModel (Ver. 8.6) modeling package⁶ were performed. Conformational searching was carried out by using the MCMM (torsional sampling Monte Carlo multiple minimum) option, and each random conformation was minimized using the Polak-Ribiere Conjugate Gradient method (PRCG) with the MM3^{*} force field. The minimization convergence criteria were considered to be complete when the gradient was less than 0.005. For each compound the conformational analyses always found both 1,3-alternate conformation (*syn*-isomer) and chair conformation (*anti*-isomer) among the output structure collected within 80 kJ mol⁻¹. The calculated steric energy differences (ΔE kJ mol⁻¹) between the *anti*- and *syn*-isomer of **6** are reported in Table 2. For comparison, the ΔE values for the corresponding oxacalix[4]arenes **7** bearing no *tert*-butyl substituents are also included in this table. In all cases, the *syn*-isomers are more stable than the *anti*-isomers. In the series of **6**, the *anti*-isomers have energy higher by 53–72 kJ mol⁻¹ than the corresponding *syn*-isomers. Thus, it is reasonable to postulate that the preferred formation of *syn*-isomers is accounted for by these energy differences. On the other hand, in the series of **7**, the ΔE values are in the range of 6–15 kJ mol⁻¹. In the case of compounds **7a** and **7c**, only the *syn*-isomers were isolated in the K₂CO₃/DMSO, CsF/DMF or Et₃N/MeCN system; whereas the base-catalyzed synthesis of **7b** and **7d** produced a mixture of the two isomers, and the *anti*-isomers readily converted to the thermodynamically more stable *syn*-isomers in the presence of K₂CO₃ or CsF. The reason for the *syn*-preference in the synthesis of **6** is that the energy gap between the *syn*-isomer and *anti*-isomer much increased by introducing *tert*-butyl groups at the extra-annular *ortho* positions relative to the bridging oxygen atoms.

2.2. X-ray crystal structures

All oxacalix[4]arenes **6a–d** adopt unsymmetrical 1,3-alternate conformations. Figure 1 shows the ORTEP drawing of their crystal structures. Their conformational features are characterized by the following structural parameters. As shown in Scheme 4, four benzene rings are designated as *a*, *b*, *c* and *d* and the mean plane defined by the bridging four oxygen atoms is designated as *m*. The parameters are: the deviation of the bridging oxygen atoms from



Scheme 4. Structural parameters for **6** (R=*tert*-Bu) and **7** (R=H).

the mean plane *m*; the dihedral angles between the aromatic rings and the mean plane, (*a/m*), (*b/m*), (*c/m*), (*d/m*); the centroid...centroid distances between the opposite aromatic rings, (*a-c*), (*b-d*); the average bond length between the bridging oxygen atom and the dinitrobenzene (*l_n*), and the average bond length between the bridging oxygen atom and the di-*tert*-butylbenzene ring (*l_b*). These relevant structural parameters are summarized in Table 3. For comparison, the parameters for the oxacalix[4]arenes **7b**,^{2b} **7c**⁴ bearing no *tert*-butyl substituents are also listed in this table.

Table 3
Structural parameters of oxacalix[4]arenes **6** and **7**

	6a	6b	6c	6d	7b	7c
Deviation of the bridging oxygen atoms from the mean plane (Å)						
	0.305	0.019	0.020	0.108	0.095	0.038
	-0.307	-0.019	-0.020	-0.108	-0.096	-0.038
	0.304	0.020	0.020	-0.108	0.095	0.038
	-0.306	-0.020	-0.020	-0.108	-0.095	-0.038
Dihedral angles between the di- <i>tert</i> -butylbenzene rings and the mean plane (°)						
<i>a/m</i>	57.9	77.2	77.4	76.6	87.7	81.7
<i>c/m</i>	57.9	77.5	73.3	74.3	88.2	87.8
Dihedral angles between the dinitrobenzene rings and the mean plane (°)						
<i>b/m</i>	64.9	35.2	35.3	37.5	17.0	18.8
<i>d/m</i>	64.4	38.9	39.0	47.7	28.1	36.1
Centroid...centroid distances (Å)						
<i>a-c</i>	6.081	5.333	5.339	5.324	4.755	4.905
<i>b-d</i>	5.676	6.808	6.782	6.712	7.317	7.108
Average bond lengths (Å)						
<i>l_n</i>	1.360	1.353	1.356	1.356	1.358	1.356
<i>l_b</i>	1.401	1.408	1.405	1.400	1.414	1.398

In the crystal of compound **6a**, there is one DMF molecule between the opposite di-*tert*-butylbenzene rings. One of the methyl groups of the DMF molecule is pointing toward the mean plane *m* and is located nearly above the centroid of the nearer di-*tert*-butylbenzene ring. The inclusion of the DMF molecule probably forces the macrocycle **6a** to bend and to open the cavity. Indeed, the deviation of the bridging oxygen atoms from the mean plane *m* is 0.30 Å. This value is much larger than that of **6b** (0.02 Å), **6c** (0.02 Å) and **6d** (0.11 Å). Furthermore, **6a** has the longest centroid...centroid distance (*a-c*) and the shortest centroid...centroid distance (*b-d*) among the oxacalix[4]arenes investigated. The distance between the carbon of the methyl group and the aromatic ring is 3.64 Å, indicating some C-H... π interactions.

The crystal structures of **6b**, **6c**, and **6d** resemble each other. The four bridging oxygen atoms are located nearly in the mean plane *m* described as above. The dihedral angles *a/m* and *c/m* are in the range of 73.3–77.5°, and the dihedral angles *b/m* and *d/m* are in the range of 35.2–47.7°. The centroid...centroid distances *a-c*, *b-d* are in the range of 5.32–5.34 Å and 6.71–6.81 Å, respectively. The substituents (Me, OH, COOMe) at the intra-annular positions have little effect on the conformational preference of the oxacalix[4]arenes. For compound **6c**, there is no hydrogen bonding between the distal OH groups, because the O...O distance of 4.25 Å is much longer than that of usual hydrogen bonded O...O distance (ca. 2.85 Å). For compound **6d**, the ester groups are arranged in antiparallel fashion with respect to each other, and the oxygen atoms of the carbonyl groups point inward of the cavity. The torsion angles between the planes of the ester groups and the aromatic ring bearing the substituent are 40.8° and 37.6°. This torsion of the ester groups is apparently due to steric interaction with the dinitrobenzene rings. For the oxacalix[4]arenes **7b** and **7c**, bearing no *tert*-butyl substituents, the dihedral angles *a/m* and *c/m* are in the range of 81.7–88.9°, the dihedral angles *b/m* and *d/m* are in the range of 17.0–36.1°, and the centroid...centroid distances *a-c*, *b-d* are in the range of 4.76–4.91 Å and 7.11–7.32 Å, respectively. Obviously, the centroid...centroid distances *a-c* are elongated by the introduction of the four *tert*-butyl substituents at the extra-annular

positions. Concurrently, the centroid–centroid distances *b–d* are shortened by this modification.

In these compounds, the bonds between the bridging oxygen atom and the dinitrobenzene ring are shorter than the bond between the bridging heteroatom and the di-*tert*-butylbenzene rings. The significant shortening of the former bonds indicate that the bridging oxygen atoms strongly conjugate with the dinitrobenzene rings. For all compounds, these bond lengths and the differences ($l_n - l_b$) are similar. Hence it is considered that the *tert*-butyl substituents do not influence the conjugation between the bridging oxygen atoms with the dinitrobenzene rings.

3. Conclusion

In the present study, we accomplished the preparation of oxalix[4]arenes **6** by aromatic nucleophilic substitution of 1,5-difluoro-2,4-dinitrobenzene with 4,6-di-*tert*-butylresorcinols. ¹H NMR and X-ray crystallographic analysis demonstrated that the oxalix[4]arenes adopt 1,3-alternate conformations both in solution and in the solid state. Introduction of four *tert*-butyl groups at the *ortho* position to the bridging oxygen atoms inhibits the C–O bond cleavage via *ipso*-attack of nucleophiles. Furthermore, the substituents enhance the solubility of the macrocycles in common organic solvents. The presence of nitro functions will allow the design of novel building blocks for host molecules. Preparation of derivatives of this type is the subject of our investigation.

4. Experimental section

4.1. General

Melting points were determined with a Laboratory Devices Mel-Temp II capillary melting point apparatus and are uncorrected. Elemental analyses were performed at the Division of Instrumental Analysis, Research Center for Bioscience and Technology, Tottori University. Preparative gel permeation liquid chromatography (GPLC) was performed on a Japan Analytical Industry LC-918 instrument equipped with refractive index detector RI-50, using chloroform as a mobile phase on JAI gel 1H+2H columns (20×600 mm). ¹H and ¹³C NMR spectra were recorded in CDCl₃ or DMSO-*d*₆ solution with a JEOL JNM LA400 or a JEOL JNM ECP500 spectrometer. All chemical shifts are quoted in parts per million on the δ scale with TMS or residual solvent signal as an internal standard. Fast atom bombardment mass spectra were recorded using xenon ionization techniques with *m*-nitrobenzyl alcohol (MNBA) as the matrix on a JEOL AX-505 spectrometer at the Faculty of Agriculture, Tottori University. Infrared spectra were recorded with KBr discs using a Perkin Elmer FT-IR 1600 spectrometer.

4.2. Synthesis of oxalix[4]arenes

1,5-Difluoro-2,4-dinitrobenzene **1** (1 mmol), the appropriate resorcinol (1 mmol), and CsF (2 mmol) were combined in a round-bottomed flask under an argon atmosphere. Dry DMF (2.5 ml) was added, and the reaction mixture was then stirred for 2 h at 100 °C. After cooling, dilution of the mixture with methanol/water (1:1 v/v) produced light tan precipitates, which were collected by filtration, washed with water, then methanol, and finally dried under reduced pressure. The crude product was purified by GPC and recrystallization from appropriate solvents.

4.2.1. *1*⁴,*1*⁶,*5*⁴,*5*⁶-Tetra-*tert*-butyl-*3*⁴,*3*⁶,*7*⁴,*7*⁶-tetranitro-2,4,6,8-tetraoxa-1,3,5,7(1,3)-tetrabenzenacyclooctaphane (**6a**). The crude product was purified by recrystallization from CHCl₃/hexane to produce a tan powder. (74%); mp 310 °C (dec). R_f =0.8 (hexane/EtOAc 3:1). Anal. Calcd for C₄₀H₄₄N₄O₁₂: C, 62.17; H, 5.74; N, 7.25.

Found: C, 62.03; H, 5.85; N, 7.09. 400 MHz ¹H NMR (CDCl₃, 30 °C) δ 1.31 (s, 36H, *t*-Bu), 6.16 (s, 2H, *meta* to NO₂), 6.48 (s, 2H, *meta* to *t*-Bu), 7.53 (s, 2H, *ortho* to *t*-Bu), 8.83 (s, 2H, *ortho* to NO₂). 125 MHz ¹³C NMR (CDCl₃, 30 °C) δ 30.1, 35.0, 105.6, 114.6, 126.0, 128.0, 133.3, 140.3, 150.5, 156.0. IR (KBr) cm⁻¹ 2965, 1618, 1597, 1533, 1350, 1296.

4.2.2. *1*²,*5*²-Dimethyl-*1*⁴,*1*⁶,*5*⁴,*5*⁶-tetra-*tert*-butyl-*3*⁴,*3*⁶,*7*⁴,*7*⁶-tetranitro-2,4,6,8-tetraoxa-1,3,5,7(1,3)-tetrabenzenacyclooctaphane (**6b**). GPC separation and recrystallization from CHCl₃/hexane yielded **6b** as a colorless solid (70%); mp 250 °C (dec). R_f =0.8 (hexane/EtOAc 3:1). Anal. Calcd for C₄₂H₄₈N₄O₁₂: C, 62.99; H, 6.04; N, 7.00. Found: C, 63.00; H, 6.09; N, 6.96. FABMS m/z 800 (M⁺). 400 MHz ¹H NMR (CDCl₃, 30 °C) δ 1.26 (s, 36H, *t*-Bu), 1.72 (s, 6H, Me), 5.73 (s, 2H, *meta* to NO₂), 7.41 (s, 2H, *ortho* to *t*-Bu), 8.91 (s, 2H, *ortho* to NO₂). 125 MHz ¹³C NMR (CDCl₃, 30 °C) δ 11.5, 30.5, 35.3, 102.2, 123.3, 125.3, 126.5, 131.8, 140.8, 148.2, 156.0. IR (KBr) cm⁻¹ 2967, 1614, 1599, 1532, 1478, 1348, 1298.

4.2.3. *1*²,*5*²-Dihydroxy-*1*⁴,*1*⁶,*5*⁴,*5*⁶-tetra-*tert*-butyl-*3*⁴,*3*⁶,*7*⁴,*7*⁶-tetranitro-2,4,6,8-tetraoxa-1,3,5,7(1,3)-tetrabenzenacyclooctaphane (**6c**). GPC separation and recrystallization from CHCl₃/hexane yielded **6c** as a colorless solid (27%); mp 305 °C (dec). R_f =0.6 (hexane/EtOAc 3:1). Anal. Calcd for C₄₀H₄₄N₄O₁₄·2H₂O: C, 57.14; H, 5.75; N, 6.66. Found: C, 57.22; H, 5.82; N, 6.57. 500 MHz ¹H NMR (CDCl₃, 30 °C) δ 1.38 (s, 36H, *t*-Bu), 5.24 (br, 2H, OH), 6.00 (s, 2H, *meta* to NO₂), 7.05 (s, 2H, *ortho* to *t*-Bu), 8.83 (s, 2H, *ortho* to NO₂). 125 MHz ¹³C NMR (CDCl₃, 30 °C) δ 30.3, 35.4, 103.2, 117.3, 125.6, 132.3, 138.9, 139.8, 141.0, 155.9. IR (KBr) 3524, 2963, 1618, 1597, 1529, 1354, 1298 cm⁻¹.

4.2.4. Dimethyl-*1*⁴,*1*⁶,*5*⁴,*5*⁶-tetra-*tert*-butyl-*3*⁴,*3*⁶,*7*⁴,*7*⁶-tetranitro-2,4,6,8-tetraoxa-1,3,5,7(1,3)-tetrabenzenacyclooctaphane-*1*²,*5*²-dicarboxylate (**6d**). GPC separation and recrystallization from CHCl₃/hexane yielded **6d** as a colorless solid (49%); mp 255 °C (dec). R_f =0.6 (hexane/EtOAc 3:1). Anal. Calcd for C₄₄H₄₈N₄O₁₆: C, 59.45; H, 5.44; N, 6.30. Found: C, 59.50; H, 5.36; N, 6.32. 400 MHz ¹H NMR (CDCl₃, 30 °C) δ 1.31 (s, 36H, *t*-Bu), 3.43 (s, 6H, CH₃), 5.65 (s, 2H, *meta* to NO₂), 7.70 (s, 2H, *ortho* to *t*-Bu), 8.82 (s, 2H, *ortho* to NO₂). 125 MHz ¹³C NMR (CDCl₃, 30 °C) δ 30.5, 35.7, 52.7, 104.3, 119.6, 125.1, 130.4, 132.3, 141.8, 148.9, 157.1, 161.5. IR (KBr) 2965, 2876, 1734, 1616, 1530, 1352, 1304 cm⁻¹.

4.3. Crystal structure determination

Intensity data and cell parameters were recorded on a Rigaku RAXIS RAPID imaging plate area detector with graphite monochromated Mo K α radiation (λ =0.7107 Å). Calculations were performed using the WinGX⁷ (for **6a** and **7d**) or the CrystalStructure⁸ (for **6b**, **6c**, and **6d**). The structure was solved by direct methods and refined by full-matrix, least-squares procedures (based on F_o^2), using of the SHELXL-97 program.⁹ Crystallographic data in cif format can be obtained free of charge from The Cambridge Crystallographic Data Centre via www.ccdc.cam.ac.uk/data_request/cif.

4.3.1. Crystallographic data for compound 6a. Diffraction-quality crystals were obtained by slow vapor diffusion of water to DMF: C₄₀H₄₄N₄O₁₂·C₃H₇NO, M =845.89, crystal size: 0.3×0.3×0.3 mm³, crystal system: monoclinic, space group: Cc, a =21.798(15), b =9.700(9), c =20.683(8) Å, α =90°, β =94.99(2)°, γ =90°, volume: 4356(5) Å³, Z =4, T =173 K, ρ (calcd)=1.29 g·cm⁻³, $F(000)$ =1792, 34,254 reflections collected, 9017 unique (R_{int} =0.030). A DMF molecule is disordered in a ratio of 0.5 to 0.5 about the twofold axis perpendicular to the mean plane of the macrocycle. All heavy atoms were refined anisotropically. Hydrogen atoms were placed from expected geometry and refined isotropically. This model converged to the final R_1 =0.0365, wR_2 =0.0993 and GOF=0.922 with 595

parameters. Residual peaks in final difference map were $0.21 \text{ e} \text{ \AA}^{-3}$ and $-0.21 \text{ e} \text{ \AA}^{-3}$. CCDC reference number 740949.

4.3.2. Crystallographic data for compound 6b. Single crystals were obtained by vapor diffusion of hexane in a CHCl_3 solution at room temperature: $\text{C}_{42}\text{H}_{48}\text{N}_4\text{O}_{12}$, $M=808.86$, crystal size: $0.5 \times 0.5 \times 0.2 \text{ mm}^3$, crystal system: triclinic, space group: $P-1$, $a=11.449(1)$, $b=13.687(1)$, $c=13.873(1) \text{ \AA}$, $\alpha=74.55(1)^\circ$, $\beta=79.70(1)^\circ$, $\gamma=87.71(1)^\circ$, volume: $2062(1) \text{ \AA}^3$, $Z=2$, $T=173 \text{ K}$, $\rho(\text{calcd})=1.290 \text{ g cm}^{-3}$, $F(000)=848$, 19,964 reflections collected, 9339 unique ($R_{\text{int}}=0.019$). All heavy atoms were refined anisotropically. Hydrogen atoms were placed from expected geometry and refined isotropically. This model converged to the final $R_1=0.0435$, $wR_2=0.1414$ and $\text{GOF}=1.026$ with 548 parameters. Residual peaks in final difference map were $0.53 \text{ e} \text{ \AA}^{-3}$ and $-0.41 \text{ e} \text{ \AA}^{-3}$. CCDC reference number 740950.

4.3.3. Crystallographic data for compound 6c. Single crystals were obtained by vapor diffusion of hexane in a CHCl_3 solution at room temperature: $\text{C}_{40}\text{H}_{44}\text{N}_4\text{O}_{14}$, $M=804.81$, crystal size: $0.5 \times 0.2 \times 0.1 \text{ mm}^3$, crystal system: triclinic, space group: $P-1$, $a=11.432(3)$, $b=13.655(5)$, $c=13.883(5) \text{ \AA}$, $\alpha=74.69(1)^\circ$, $\beta=79.56(1)^\circ$, $\gamma=87.49(1)^\circ$, volume: $2056(1) \text{ \AA}^3$, $Z=2$, $T=173 \text{ K}$, $\rho(\text{calcd})=1.300 \text{ g cm}^{-3}$, $F(000)=848$, 19,962 reflections collected, 9273 unique ($R_{\text{int}}=0.058$). All heavy atoms were refined anisotropically. Positions of the OH hydrogen were located by the direct method. Hydrogen atoms of eight methyl groups in four *tert*-butyl groups were placed using an idealized disordered CH_3 model. Other hydrogen atoms were placed from expected geometry. All hydrogen atoms were refined isotropically. This model converged to the final $R_1=0.0754$, $wR_2=0.2096$ and $\text{GOF}=1.063$ with 524 parameters. Residual peaks in final difference map were $0.47 \text{ e} \text{ \AA}^{-3}$ and $-0.67 \text{ e} \text{ \AA}^{-3}$. CCDC reference number 740951.

4.3.4. Crystallographic data for compound 6d. Single crystals were obtained by vapor diffusion of hexane in an acetone solution at room temperature: $\text{C}_{44}\text{H}_{48}\text{N}_4\text{O}_{16} \cdot \text{C}_3\text{H}_6\text{O}$, $M=946.96$, crystal size: $0.4 \times 0.4 \times 0.3 \text{ mm}^3$, crystal system: triclinic, space group: $P-1$, $a=13.011(5)$, $b=13.967(6)$, $c=14.257(5) \text{ \AA}$, $\alpha=71.28(2)^\circ$, $\beta=75.58(2)^\circ$, $\gamma=79.18(1)^\circ$, volume: $2360(2) \text{ \AA}^3$, $Z=2$, $T=173 \text{ K}$, $\rho(\text{calcd})=1.332 \text{ g cm}^{-3}$, $F(000)=1000$, 20,924 reflections collected, 10,464 unique ($R_{\text{int}}=0.065$). All heavy atoms were refined anisotropically.

Hydrogen atoms of eight methyl groups in four *tert*-butyl groups were placed using an idealized disordered CH_3 model and other hydrogen atoms were placed from expected geometry and were refined isotropically. Disorder of one nitro group was modeled. This model converged to the final $R_1=0.0726$, $wR_2=0.2389$ and $\text{GOF}=0.929$ with 637 parameters. Residual peaks in final difference map were $0.30 \text{ e} \text{ \AA}^{-3}$ and $-0.33 \text{ e} \text{ \AA}^{-3}$. CCDC reference number 740948.

Supplementary data

Supplementary data associated with this article can be found in online version at doi:10.1016/j.tet.2009.09.116.

References and notes

- (a) Vysotsky, M.; Saadioui, M.; Böhmer, V. In *Calixarenes 2001*; Asfari, Z., Böhmer, V., Harrowfield, J., Vicens, J., Eds.; Kluwer: Dordrecht, 2001; Chapter 13, pp. 250–265; (b) Maes, W.; Dehaen, W. *Chem. Soc. Rev.* **2008**, 37, 2393–2402; (c) Wang, M. X. *Chem. Commun.* **2008**, 4541–4551.
- (a) Wang, M. X.; Yang, H. B. *J. Am. Chem. Soc.* **2004**, 126, 15412–15422; (b) Katz, J. L.; Feldman, M. B.; Conry, R. R. *Org. Lett.* **2005**, 7, 91–94; (c) Konishi, H.; Tanaka, K.; Teshima, Y.; Mita, T.; Morikawa, O.; Kobayashi, K. *Tetrahedron Lett.* **2006**, 47, 4041–4044; (d) Katz, J. L.; Feldman, M. N.; Conry, R. R. *Org. Lett.* **2006**, 8, 2755–2758; (e) Maes, W.; Van Rossom, W.; Van Hecke, K.; Van Meervelt, L.; Debaen, W. *Org. Lett.* **2006**, 8, 4161–4164; (f) Wang, Q. Q.; Wang, D. X.; Zhang, Q. Y.; Wang, M. X. *Org. Lett.* **2007**, 9, 2847–2850.
- (a) Katz, J. L.; Selby, K. J.; Conry, R. R. *Org. Lett.* **2005**, 7, 3505–3507; (b) Hao, E.; Fronczek, F. R.; Graça, M.; Vicente, H. *J. Org. Chem.* **2006**, 71, 1233–1236; (c) Csokal, V.; Kulik, B.; Bitter, I. *Supramol. Chem.* **2006**, 18, 111–115; (d) Jiao, L.; Hao, E.; Fronczek, F. R.; Smith, K. M.; Graça, M.; Vicente, H. *Tetrahedron* **2007**, 63, 4011–4017; (e) Hou, B. Y.; Zheng, Q. Y.; Wang, D. X.; Wang, M. X. *Tetrahedron* **2007**, 63, 10801–10808; (f) Hou, B. Y.; Wang, D. X.; Yang, H. B.; Zheng, Q. Y.; Wang, M. X. *J. Org. Chem.* **2007**, 72, 5218–5226; (g) Ferrini, S.; Fusi, S.; Giorgi, G.; Ponticelli, F. *Eur. J. Org. Chem.* **2008**, 5407–5413; (h) Van Rossom, W.; Maes, W.; Kishore, L.; Ovaere, L.; Van Meervelt, L.; Debaen, W. *Org. Lett.* **2008**, 10, 585–588; (i) Hou, B. Y.; Zheng, Q. Y.; Wang, D. X.; Huang, Z. T.; Wang, M. X. *Chem. Commun.* **2008**, 3864–3866.
- Konishi, H.; Mita, T.; Yasukawa, Y.; Morikawa, O.; Kobayashi, K. *Tetrahedron Lett.* **2008**, 49, 6831–6834.
- Konishi, H.; Mita, T.; Morikawa, O.; Kobayashi, K. *Tetrahedron Lett.* **2007**, 48, 3029–3032.
- MacroModel, Version 8.6*; Schrödinger, LLC: New York, NY, 2004.
- Farrugia, L. J. *J. Appl. Crystallogr.* **1999**, 32, 837–838.
- CrystalStructure, Version 3.8.2*; Rigaku and Rigaku/MS: The Woodlands, TX, 2007.
- Sheldrick, G. M. *Acta Crystallogr., Sect. A* **2008**, 64, 112–122.